A novel treatment strategy utilizing panobinostat for high-risk and treatment-refractory hepatoblastoma
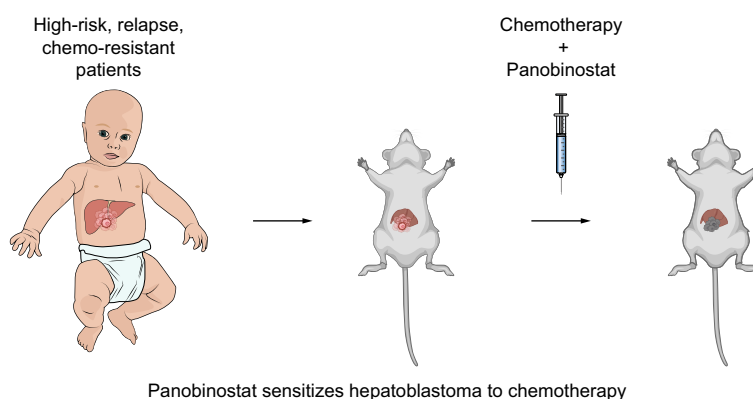
Authors

Andres F. Espinoza, Roma H. Patel, Kalyani R. Patel, …, Dolores H. López-Terrada, Sarah E. Woodfield, Sanjeev A. Vasudevan

Correspondence

sanjeevv@bcm.edu (S.A. Vasudevan).

Graphical abstract

High-risk, relapse, chemo-resistant patients

Chemotherapy
+
Panobinostat

Panobinostat sensitizes hepatoblastoma to chemotherapy

Highlights

- Combination of vincristine, irinotecan, and panobinostat causes a reduction in tumor size in pre-clinical models of hepatoblastoma.

- We developed a clinically relevant pipeline that can be used to screen novel targeted therapies.

- PDX drug testing utilizing the VI backbone has the potential to create novel treatment strategies.

Impact and implications

Patients with treatment-refractory hepatoblastoma have limited treatment options with survival rates of less than 50%. Our manuscript demonstrates that combination therapy with vincristine, irinotecan, and panobinostat reduces the size of high-risk, relapsed, and treatment-refractory tumors. With this work we provide preclinical evidence to support utilizing this combination therapy as an arm in future clinical trials.

A novel treatment strategy utilizing panobinostat for high-risk and treatment-refractory hepatoblastoma

Andres F. Espinoza[1], Roma H. Patel[1], Kalyani R. Patel[2], Andrew A. Badachhape[3], Richard Whitlock[1], Rohit K. Srivastava[1], Saiabhiroop R. Govindu[1], Ashley Duong[1], Abhishek Kona[1], Pavan Kureti[1], Bryan Armbruster[1], Dina Kats[4], Ramakrishnan R. Srinivasan[5], Lacey E. Dobrolecki[5], Xinjian Yu[6], Mohammad J. Najaf Panah[6], Barry Zorman[6], Stephen F. Sarabia[2], Martin Urbicain[2], Angela Major[2], Karl-Dimiter Bissig[7], Charles Keller[4], Michael T. Lewis[5], Andras Heczey[6], Pavel Sumazin[6], Dolores H. López-Terrada[2], Sarah E. Woodfield[1], Sanjeev A. Vasudevan[1,*]

Check for updates

Background & Aims: Patients with metastatic, treatment-refractory, and relapsed hepatoblastoma (HB) have survival rates of less than 50% due to limited treatment options. To develop new therapeutic strategies for these patients, our laboratory has developed a preclinical testing pipeline. Given that histone deacetylase (HDAC) inhibition has been proposed for HB, we hypothesized that we could find an effective combination treatment strategy utilizing HDAC inhibition.

Methods: RNA sequencing, microarray, NanoString, and immunohistochemistry data of patient HB samples were analyzed for HDAC class expression. Patient-derived spheroids (PDSp) were used to screen combination chemotherapy with an HDAC inhibitor, panobinostat. Patient-derived xenograft (PDX) mouse models were developed and treated with the combination therapy that showed the highest efficacy in the PDSp drug screen.

Results: HDAC RNA and protein expression were elevated in HB tumors compared to normal livers. Panobinostat (IC_{50} of 0.013-0.059 μM) showed strong *in vitro* effects and was associated with lower cell viability than other HDAC inhibitors. PDSp demonstrated the highest level of cell death with combination treatment of vincristine/irinotecan/panobinostat (VIP). All four models responded to VIP therapy with a decrease in tumor size compared to placebo. After 6 weeks of treatment, two models demonstrated necrotic cell death, with lower Ki67 expression, decreased serum alpha fetoprotein and reduced tumor burden compared to paired VI- and placebo-treated groups.

Conclusions: Utilizing a preclinical HB pipeline, we demonstrate that panobinostat in combination with VI chemotherapy can induce an effective tumor response in models developed from patients with high-risk, relapsed, and treatment-refractory HB.

Introduction

Hepatoblastoma (HB) is the most common liver cancer in children, comprising one percent of all pediatric malignancies.[1] While low-risk disease responds well to the multidisciplinary approach of perioperative chemotherapy and surgery, high-risk disease continues to lead to high rates of relapse and mortality.[2] Additionally, histologically aggressive cases of HB in older children have been characterized to have mutations commonly observed in hepatocellular carcinoma (HCC) and may benefit from specialized treatment strategies.[3] In response, institutes have proposed the combination of vincristine and irinotecan (VI) as a salvage therapy for these scenarios.[4] While evidence exists for initial response to the VI strategy, many patients are refractory to this treatment and succumb to disease progression.[4] Additionally, current standard of care chemotherapy is associated with risks of lifelong deafness and cardiac dysfunction.[1,4] Thus, new therapies against relapsed-refractory and high-risk HB are needed.

Patient-derived xenograft (PDX) mouse models are important tools that have contributed to our understanding of many aspects of human cancer biology.[5] Despite this, major obstacles have prevented the standardization of clinically relevant models. First, the length of time to engraft PDXs can be in the order of months.[5] With this timeframe, many patients succumb to their malignancy or are treated with other regimens. In addition, most HB PDX tumors are subcutaneously implanted in the flank and thus are limited in their relevancy.[5] Mice are also started on therapies with small tumor sizes to attempt slowing of growth, also limiting their applicability.[5] Finally, preclinical testing of targeted monotherapy has led to very few effective therapies for pediatric solid tumors in general, emphasizing the need for combination testing with current chemotherapies.[6–9] Thus, an efficient combinatorial chemotherapy testing pipeline that provides clinically relevant HB models is warranted.

HDAC inhibitors (HDACi) have gained attention as possible agents for the treatment of cancer, with significant treatment

advances in hematological malignancies.[10] Panobinostat, a pan-HDAC class inhibitor has been studied in multiple clinical trials for use in children with both solid and hematological malignancies, showing that the drug is well tolerated with a low toxicity profile.[10,11] Despite previous studies suggesting HDACi may provide treatment options in HB, there is no published data on panobinostat combination therapies being tested in a preclinical pipeline platform for HB.[12–14] We hypothesized that panobinostat would show efficacy in combination with the salvage chemotherapy regimen VI for relapse-refractory and high-risk HB.

Materials and methods

Patient-derived cell line

HB17, our patient-derived cell line was established in our laboratory by plating dissociated cells from a patient sample on 6 cm culture plates coated with Corning Matrigel GFR Membrane Matrix Matrigel (cat. no. CB-40234, Thermo Fisher Scientific, Waltham, MA, USA). These were passaged every 2 weeks and after 20 passages were weaned off Matrigel. After passage 49 they were able to be maintained in 50% MEM and 50% HBM media (cat. no. CC-3198 Lonza, Walkerville, MD, USA). For our experiments we used passage #52-54. For the validation of HB17 we performed a single tandem repeat (STR) assay (Supplementary Material 1) and serum human alpha fetoprotein (AFP) levels, a marker for HB, were confirmed to be elevated (>100 ng/ml), using the ELISA (EIA-1468, DRG Instruments, Germany), before performing experiments.

Drug screen

HB cells were plated after trypsinization into a 384-well plate containing pre-diluted drugs. Cell-Titer Glo 2.0 (cat. no. G9243, Promega, Madison, WI, USA) was added to each cell well and was evaluated after rocking in the dark for 15 min. Cells were kept at room temperature throughout the entire experiment. The plate luminescence was evaluated utilizing BioTek Synergy HT Microplate Reader (BioTek, Charlotte, VT, USA) as described in Kats *et al.* 2019.[15]

Patient-derived spheroid (PDsp) techniques

Freshly obtained 1 cm tumors were washed and dissociated using scissors and the back of a 10 ml syringe. Dissociated tissue was washed twice with 1x PBS and red blood cells were lysed with 5 ml of ACK Lysing buffer (cat. no. A10492, Thermo Fisher Scientific, Waltham, WA, USA) for 5 min on ice. Cells were washed by adding 40 ml of 1x PBS and centrifuged at 300 g for 10 min. Supernatant was removed and 10 ml of 1x PBS was added to the tissue with 1 ml of dispase (071913, Stemcell, Vancouver, CA), 200 μl of 2 mg/ml collagenase and 100 μl of DNase (cat. no. 04716728001, Sigma-Aldrich, St. Louis, MO, USA). This was then placed in a 37°C-water bath for 30 min. Tissue was vortexed every 5 min. Tissue/cells were filtered using a 70 μm filter. Filtered cells were washed twice with 30 ml of 1x PBS. Pelleted cells were re-suspended in 5 ml of HBM media (cat. no. CC-3198, HCM bullet kit, Lonza, Walkerville, MD, USA). Cells were counted and 10,000 cells/well were plated in 96 well Nunclon Sphere round bottom plates (cat. no. 174925, Thermo Fisher Scientific, Waltham, WA, USA) in 100 μl of HBM media and 1 μm of Y-27632 (cat. no. 1254, Tocris Biosciences, Bristol,

UK). Plates were spun at 300 g for 5 min. Plates were maintained in a humidified incubator at 37 °C and 5% CO_2 for 11 days with 25 μl media added to each well on day 5 and day 9. At day 11 all standard chemotherapies were added at 0.05 μM for low dose and 0.1 μM for high dose. Panobinostat was used at 0.01 for low dose and 0.05 μM dose for high dose in all combination studies. Drugs were added for 48 h, and cell viability was measured using CellTiter-Glo 3D Cell Viability Assay using a 96-well plate luminometer (cat. no. G9681, Promega, Madison, WI, USA). Panobinostat (LBH589, cat. no. S1030, Selleckchem, Houston, TX, USA), cisplatin (cat. no. S1166, Selleckchem, Houston, TX, USA), doxorubicin (cat. no. S1208, Selleckchem, Houston, TX, USA), fluorouracil (5-FU) (cat. no. S1209, Selleckchem, Houston, TX, USA), vincristine (cat. no. S9555, Selleckchem, Houston, TX, USA), and SN-38 (cat. no. S4908, Selleckchem, Houston, TX, USA) were re-suspended in DMSO to generate 10 mM stock solutions for use with PDSp.

Xenograft experiments

We obtained patient samples directly after biopsy, resection, or transplant procedures were performed according to Institutional Review Board AN-6191 at Baylor College of Medicine, Houston, TX, USA. The mice implanted with the tumor sample directly from the patient were termed P0. When the tumor began to impact animal health or when estimated tumor size by MRI reached criteria for euthanasia, as described in the approved animal protocol (AN-6191), animals were euthanized, and tumors were serially passaged into subsequent NOD scid gamma immunocompromised animals for continued growth as P1, P2, P3 etc. With these basic protocols, we were able to generate four unique aggressive models of HB. Tumors were implanted as 6-8 mm³ whole pieces into the liver of 6–12-week-old NOD scid gamma immunocompromised animals as previously described.[4] Approximately 2 weeks after implantation, animals were monitored for tumor growth with MRI and an ELISA kit (EIA-1468, DRG Instruments, Germany) to measure levels of AFP. Given that many of these patients present with advanced disease, we allowed the tumor volume to reach 0.09-0.5 cm³ to better model patient tumor burden. This volume was consistently reached and evaluated through MRI. Mice that were P2–P4 were treated with a combination of VI (vincristine [cat. no. S9555, Selleckchem, Houston, TX, USA]: 1 mg/kg, 1x a week; irinotecan [cat. no. S2217 Selleckchem, Houston, TX, USA]: 2.5 mg/kg, 5x a week, every other week), a combination of VI/panobinostat (VIP, panobinostat [cat. no. S1030, Selleckchem, Houston, TX, USA]: 8 mg/kg, 3x a week; vincristine: 1 mg/kg, 1x a week; irinotecan: 2.5 mg/kg, 5x a week, every other week), or the vehicle of the VIP therapy (Fig. S1). Panobinostat, vincristine, and irinotecan were re-suspended in DMSO to generate 62.5 mg stock solution. Panobinostat was further diluted in PEG 300, Tween 80, and sterile saline. Vincristine and irinotecan were further diluted in saline. Mice were treated for approximately 6 weeks or until they met the euthanasia event of tumor diameter of 1.5 cm. Blood was drawn for AFP level evaluation at the beginning of the study and at 3 and 6 weeks from the facial veins of mice harboring xenograft tumors. Blood was also drawn at the time a tumor reached 1.5 cm at which point mice were euthanized. Weight fold change was calculated by dividing the weight of each mouse at each week divided by the weight when the mouse was started on the drug study. The response to chemotherapy

through histology was evaluated by a pathologist (KP). GraphPad Prism (version 7.0a, GraphPad Software, Inc., La Jolla, CA, USA) was utilized to perform Student's *t* test (two-tailed) for the tumor weight and relative tumor volume with *p* >0.05 noted by not significant (n.s.) and *p* ≤0.05 noted to be significant (*). The treated to placebo ratio for each PDX model was determined by averaging the treated cohort (VI or VIP) tumor volume at the time of euthanasia compared to the average placebo tumor volume at time of euthanasia.[16] Relative tumor volume was calculated for each mouse by dividing the tumor volume at the time of euthanasia by the tumor volume at the beginning of the study per Houghton *et al.* 2012.[16] RNA was extracted from a total of 12 PDX tumors that were treated with either the vehicle of VIP treatment (placebo), VI, or VIP in each of the four PDX models tested. A tumor was chosen blindly for all three treatment groups for HB52 and HB66 at time of euthanasia. Given HB106 had no visible tumor remaining at the end of study, mice were treated with all three drug groups for 72 h, with the same treatment regimen and dose, and then euthanized. To control for this, HB113 was treated in the same manner with mice euthanized after 72 h. RNA was extracted, processed, sequenced, and analyzed as mentioned previously. Statistical significance was calculated utilizing Student's *t* test. Please refer to the CTAT table and supplementary materials and methods for additional details.

Results

HDAC expression is elevated in HB

To study the role that HDACi could play in treating HB, we re-analyzed the microarray on 51 HB tumor samples and normalized the data to six matched normal livers (Fig. 1A), previously described in Sumazin *et al.* 2017.[17] These samples were obtained from the cooperative human tissue network.[17] In addition to *HDAC1*, we noted *HDAC2, HDAC3, HDAC4, SIRT1* and *HDAC11* to be overexpressed in HB samples. All other HDAC genes were not found to be statistically overexpressed in HB samples (Fig. S2). To further validate these results on a national level, we evaluated HB samples from the Children's Oncology Group bank. We re-analyzed the published gene expression data set of all untreated HB tumor samples noted in the NanoString NCounter assay (Sumazin *et al.* 2022) and compared them to seven non-cancer-matched pediatric liver samples.[3] To note, we excluded the hepatocellular carcinoma and hepatocellular carcinoma fibrolamellar subtypes as these were noted not to have statistically significantly higher HDAC expression. Comparing this cohort, we found that *HDAC2, HDAC4, and HDAC11* were elevated in tumors compared to matched liver samples (Table 1). Given HDAC class III was not fully evaluated, we excluded class III in this analysis. Of the histological subtypes evaluated, fetal and epithelial HB appeared to have the highest relative mRNA expression of *HDAC2, HDAC4*, and *HDAC11*.

To further validate the high expression of HDAC in HB, we performed RNA sequencing on five patient tumor samples that we used to develop six PDXs (Fig. 1B). We compared these to liver samples from three patients. We found that *HDAC1, HDAC2, HDAC4, HDAC7, SIRT1*, and *HDAC11* had a statistically higher expression compared to the pooled normal livers. Of note, the PDX tumors also had similar elevated expression of these same HDAC subtypes. We then sectioned the patients'

tumors that were utilized to create our PDXs and stained them for the same HDAC subtypes that were found to have a higher fold change on RNA sequencing (Fig. 1C). We found that the average immunohistochemistry (IHC) score that the HB tumors had was higher with HDAC1, HDAC2, HDAC4, HDAC7, and HDAC11 staining compared to paired normal livers. To note SIRT1 was noted to have a similar average IHC score as paired normal livers.

Panobinostat treatment of HB cell lines and PDSp preclinical models

To evaluate the efficacy of pan-HDAC inhibition we performed a mass drug screen utilizing eight HB cell lines. The lowest cell viability that was consistently found in all eight cell lines was panobinostat, a pan-class HDACi (Fig. 2B). Given this drug screen and the fact that class I-IV HDACs were overexpressed in multiple cohorts of HB samples, we decided to perform *in vitro* cytotoxic assays utilizing several HDACi including panobinostat, vorinostat, entinostat, and mocetinostat. As shown in Fig. 2C, off the four HDACi we tested, panobinostat was noted to cause significant cell death at the lowest nano-molar doses (IC_{50} of 0.013-0.059 μM) in three commercially acquired cell lines (HuH-6, HepG2, HepT1) as well as our established treatment-refractory patient-derived cell line (HB17) (Fig. 2A). Since panobinostat had the strongest cytotoxic effect, we decided to utilize panobinostat for the remainder of our studies. At the protein level we noted strong acetylation of both H3/H4 at 24 h with an overall increase in the ratio of acetyl H3/H4 starting at 4 h of treatment with panobinostat, demonstrating that panobinostat functions through its proposed mechanism (Fig 2D and S3, Table S1). At the same time point, we noted apoptosis evidenced through PARP cleavage with an increase in the ratio of cleaved PARP to un-cleaved PARP in all four cell lines (Table S1).

Given the high degree of cell death with panobinostat, we decided to test panobinostat as monotherapy and in combination with standard and treatment-refractory chemotherapy schemes in our PDSp models. We grew PDSp from our four high-risk and relapse/refractory HB PDXs (HB52, HB66, HB106, HB113) and performed an extensive drug screen (Fig. 3) utilizing high-risk chemotherapy schemes of cisplatin/doxorubicin, cisplatin/doxorubicin/5-FU/vincristine, and VI. We then added panobinostat to each of these regimens to test the efficacy of a combination strategy. Using this screening strategy, we noted that the therapy that was consistently causing the lowest relative cell viability was VIP in three (HB52, HB66, and HB106) of our four models, with HB113 showing relative resistance to all regimens (Fig. 3).

Overview of our PDXs and our PDX pipeline

To test the role that VIP combination therapy would have on HB, we developed four unique aggressive models of HB from four high-risk, relapsed, and treatment-refractory patients (Table 2, Fig. 4A). All four models were high-risk and multifocal in nature. Of note, three of the PDXs were obtained from patients with pretreatment extent (PRETEXT) IV disease, three patients had metastatic disease, and three patients had no decrease in AFP after their neoadjuvant chemotherapy (Table 2). All tumors were also noted to have >50% viability on histology despite three samples being obtained after intense

chemotherapy. Two of our PDXs (HB52 and HB106) were obtained from VI-naïve tumors while two of our PDXs (HB66 and HB113) had been treated with 1-4 cycles of VI-based therapy at the time we obtained tissue.

After passaging these models into the second generation, termed P1, we characterized these models thoroughly using a next-generation sequencing panel examining DNA mutations and with RNA sequencing as shown in Table 2. Importantly, all mutations found in the primary patient samples were conserved

in all PDX models, and no new mutations arose in the models. We verified that the tumors growing in animals came from the primary tumors with STR validation experiments, which matched in all cases (Supplementary Material 1). We completed immunohistochemical staining of tissues from each P1 tumor with antibodies for β-catenin and glypican-3, two common markers for HB (Fig. 4B). Importantly, the PDX tumors maintained the β-catenin and glypican-3 expression patterns of the primary patient samples.
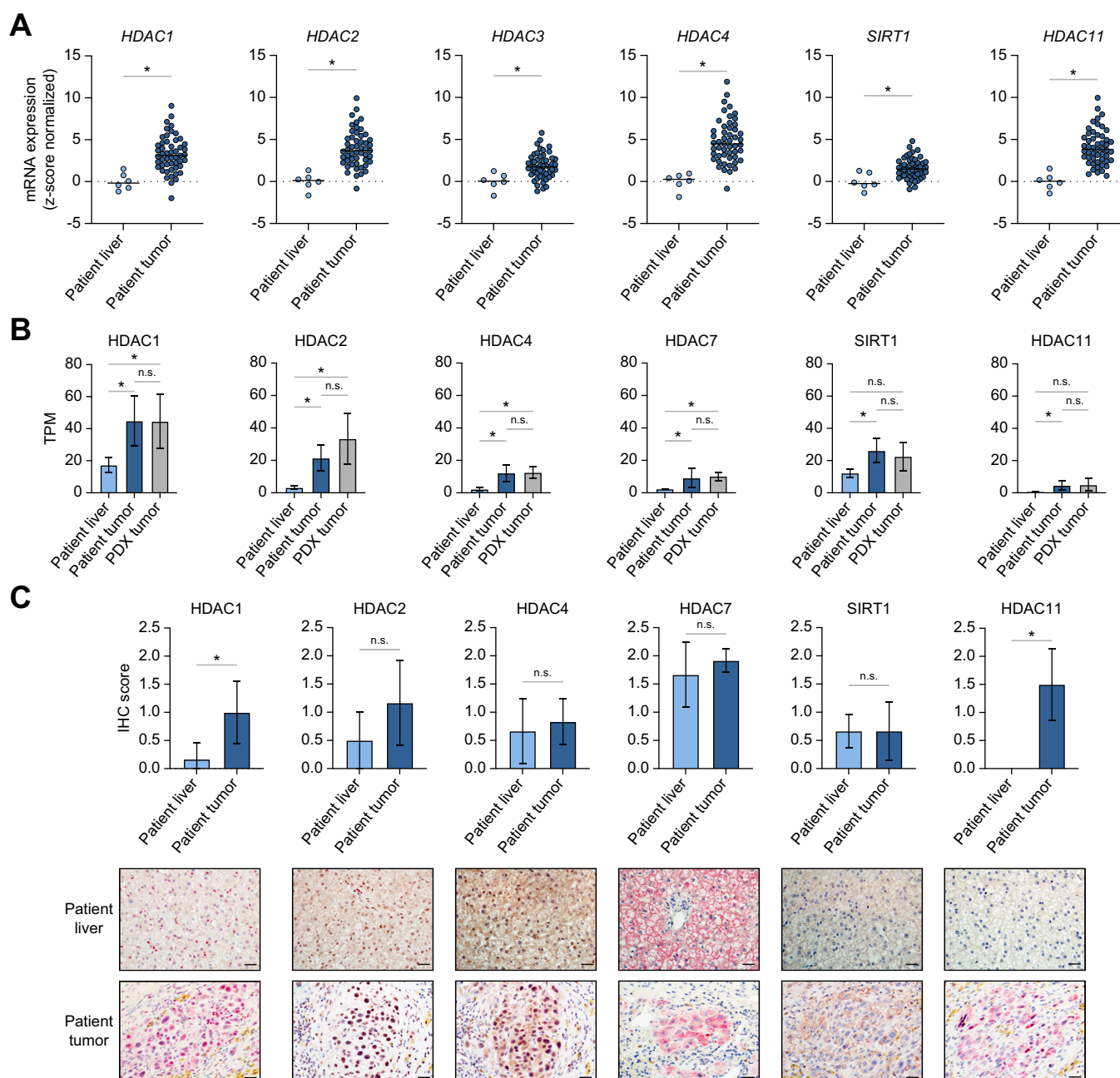

Fig. 1. HDAC gene and protein expression is elevated in HB. (A) HB patient tumors from Children's Oncology Group *HDAC* microarray expression compared to paired patient livers. (B) HDAC expression of five patients, their matched PDX tumors, and matched patient livers. (C) HDAC IHC score of six patient's primary tumors and normal livers. A representation of each HDAC of one of our PDXs is shown below to emphasize the difference between patient's HB tumors and adjacent livers. Statistical significance was calculated utilizing Student's *t* test (two-tailed) with $p \leq 0.05$ denoted by an asterisk (*) and $p > 0.05$ denoted by n.s. All histology images are taken 40x magnification with the black scale bar representing 100 μm. HB, hepatoblastoma; IHC, immunohistochemistry; PDX, patient-derived xenograft.

Table 1. NanoString *HDAC* expression and outcomes of patients with HB.

Histology	Fetal (n = 5)	Epithelial (n = 4)	Atypical (n = 6)	Biphasic HCN NOS (n = 5)	Equivocal HCN NOS (n = 9)
Age (year)	1 (IQR 0.95-1.25)	1.65 (IQR 1.2-2.05)	2.35 (IQR 1.6-6.5)	8.2 (IQR 1.85 - 17.8)	11.2 (IQR 7.75-13.5)
Sex	Female (80%)	Male (75%)	Female/male (50%)	Male (80%)	Male (66%)
TERT mutation	0%	0%	16%	60%	89%
CTNNB1 mutation	100%	100%	16%	60%	100%
Survival status	100%	50%	33%	40%	44%
HDAC2 relative expression	1.24 (p <0.01)	1.23 (p <0.01)	1.18 (p = 0.03)	1.24 (p <0.01)	1.19 (p = 0.02)
HDAC4 relative expression	1.05 (p = 0.05)	1.13 (p <0.01)	1.09 (p <0.01)	0.97 (p = 0.50)	1.06 (p = 0.02)
HDAC11 relative expression	1.17 (p <0.01)	1.14 (p = 0.03)	1.12 (p = 0.07)	0.90 (p = 0.92)	1.08 (p = 0.14)

Nanostring HDAC expression of patients separated by histology. Relative expression of each *HDAC* gene was calculated by dividing the *HDAC* expression of patient's tumors by the average *HDAC* expression of the pooled patient paired livers. Statistical significance was calculated utilizing Student's t test (two-tailed).
HB, hepatoblastoma.

Panobinostat treatment of high-risk/relapsed/refractory HB PDX models

Given the lowest relative cell viability with HB52 PDSp we chose the HB52 PDX to test panobinostat monotherapy. We found that the tumors grew at the same rate as placebos, reached event (diameter of 1.5 cm) at 1-2 weeks, and had similar tumor size at time of euthanasia as the placebo group (Fig. S4). Due to this, we deemed that panobinostat monotherapy would likely be ineffective in the remaining models. Given the lowest relative cell viability in our four PDSp models with VIP, we sought to study the role that this regimen would have on our high-risk, treatment-refractory, and relapsed HB PDXs. Initially, we decided to test HB52 given that HB52 PDSp had the lowest relative cell viability with this therapy compared to the other models. The vehicle treated mice (placebo) were noted to reach 1.5 cm diameter in 1 week. The VI-treated mice had an overall increase in tumor volume over 6 weeks, resulting in an average tumor volume fold increase of 1.8 (Fig. 5A). VIP-treated mice had significant tumor reduction after 1 week of therapy that resulted in an average volume fold decrease of 2.4 by the end of the study (Fig. 5A). AFP levels of the VIP cohort were noted to have decreased 400-fold at the 6-week mark (p = 0.05) (Fig. 5B). AFP levels decreased in the VI-treated group at 3 and 6 weeks but this change was not statistically significantly different to that in placebo mice (p = 0.07). When we repeated these experiments in HB106 we found a significant decrease in the tumors with complete disappearance of the tumors on MRI at 4 weeks, which remained until the 6-week mark (Fig. 5A), while the VI group had an average fold increase of 1.2 by the end of the study. All the HB106 placebos reached a diameter of 1.5 cm at 2 weeks. The HB106 VIP cohort similarly had an average 1.6-fold decrease in AFP compared to the 1.13-fold increase in AFP in the VI group over 6 weeks (p = 0.00019) (Fig. 5B). In HB66 and HB113, we found significant slowing down of growth with VIP compared to both placebo and VI treatment. In HB66, all the placebo-treated mice's tumors reached a diameter of 1.5 cm at 2 weeks while the VI-treated mice reached it at 3 weeks (Fig. 5C). In the VIP group, one mouse reached event at 4 weeks and another at the 6-week mark. At the 3-week mark, the HB66 VIP-treated mice had an average volume fold increase of tumor size of 3.5 while the VI group had an average volume fold increase of 11.8 (p = 0.05) (Fig. 5A). Eighty percent of the HB113 VIP cohort did not reach event over the entire 6-week study while 75% of the VI group reached event over this same period. The VIP group had a tumor volume fold increase of 4.8 while the VI group had a tumor volume fold increase of 11.7 (p = 0.11). These two PDX models did not have a decrease in AFP in either the VI or VIP

treatment arms (Fig. 5B). To note, throughout all four studies the mice were noted to have a stable body weight in all three treatment groups with no significant distress noted (Fig. S5). The tumor burden of the VIP cohort was noted to be smaller, with higher tumor signal intensity on T2 phased MRI, compared to both the placebo- and VI-treated arm for the HB52 and HB106 models (Fig. 5D,E) at the final MRI. At this time, all mice were euthanized, and their liver, lung, and tumor were harvested. Tumor burden was evident to the naked eye in all the VI- and placebo-treated arms (Fig. 5F) in all four models. At the end of the study, the HB52 and HB106 VIP cohort had no evidence of tumor on gross examination. The tumors were dissected from the native liver using the MRI image as a guide. When evaluating the tumors of all four drug studies, the relative tumor volume of the VIP group was statistically lower than that for the placebo group in three PDXs (HB52, HB106, and HB113) (Fig. S6). In addition, the treated to placebo ratio of VIP was denoted to be lower than for the VI-treated cohort in all drug studies. To validate that panobinostat functioned through its proposed mechanism on our PDX models we performed RNA sequencing and focused on mechanistic evidence using a HDAC gene signature.[18] On all four models we noted a statistically significant decrease in expression of the signature in the VIP-treated group compared to the VI-treated cohort (Fig. S7A,B, Table S2).

To elucidate the role that VIP combination therapy had at the histological level, H&E and Ki67 stains were performed. Despite there being an initial decrease in the tumors of the VI group, histologically they appeared similar to the placebo group. In contrast, the VIP-treated tumors were noted to have statistically significantly higher levels of necrosis with mesenchymal changes in HB52 and HB106 (Fig. 6A,B). The VIP-treated HB66 and HB113 mice were noted to have similar levels of necrosis as the VI cohorts but a lower percentage positivity for Ki67 (Fig. 6C,D).

Discussion

High-risk and relapsed HB continue to have poor prognosis due to ineffective therapies. Individualized therapies are warranted given the rapid rise in global incidence of HB of 4% annually, the most rapid increase seen among all pediatric solid tumors.[19] In our study we propose a new therapy scheme of VIP that is effective in treating aggressive HB subtypes *in vitro* and *in vivo*. Given our results, we believe that this therapy may be a promising and effective option for this high-risk patient cohort.

HDACs are epigenetic modulators with four separate classes that promote tumor proliferation, resistance to
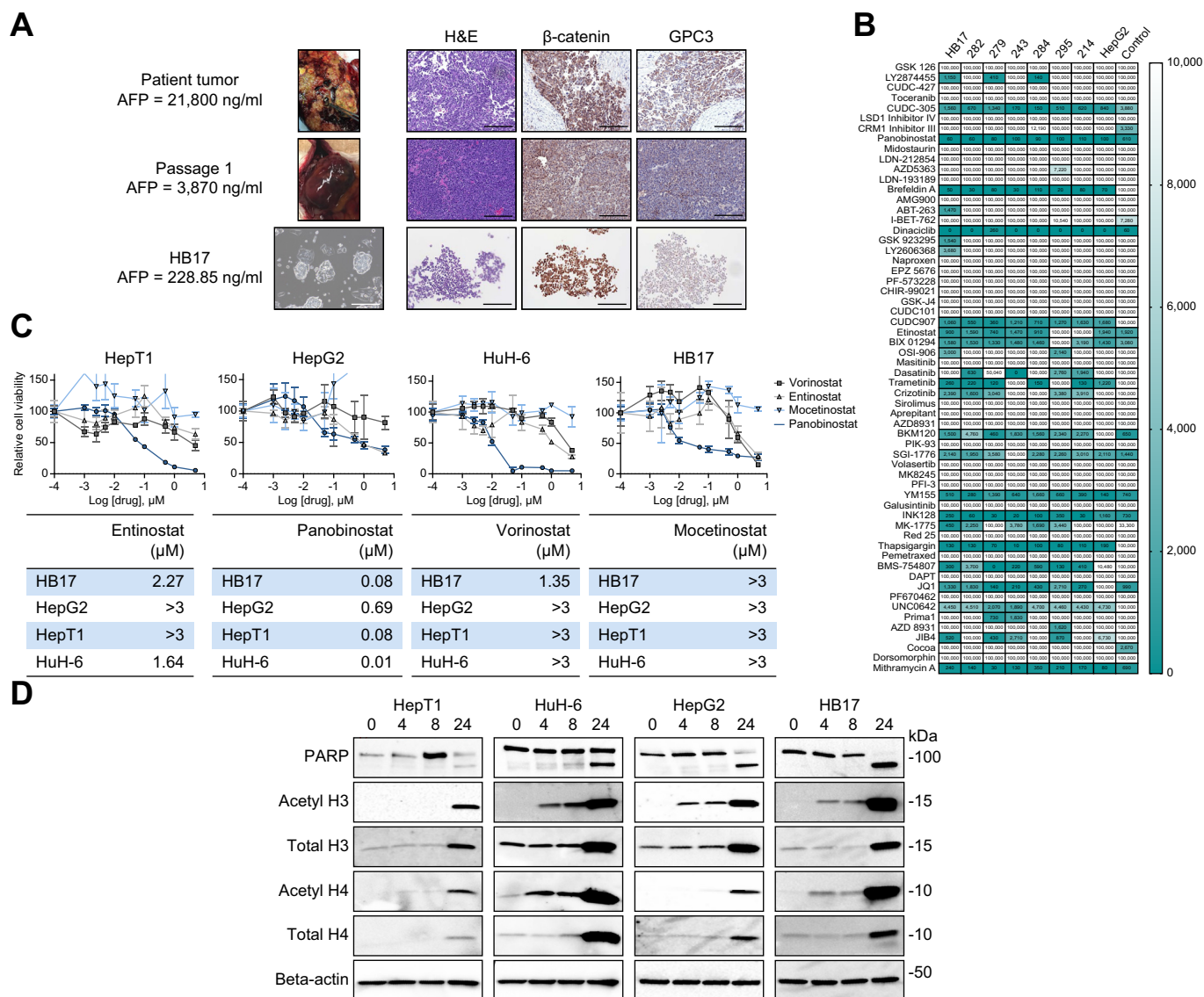
Fig. 2. Panobinostat is effective in HB in vitro. (A) To validate the HB17 cell line we compared H&E, β-catenin, and GPC3 stains from the cell line, patient tumor and PDX. AFP levels of the patient were determined at time of resection and the AFP level of the PDX and cell lines were also evaluated utilizing the ELISA kit. The PDX AFP level was calculated at time of passage (8 weeks after implantation). The cell-line AFP was calculated using 10 μl of the HB17 cell line 5 days after plating. The H&E, β-catenin, and GPC3 stain slides were taken at 20x magnification with the black scale bar representing 100 μm. The HB17 greyscale image was taken at 40x with the white scale bar representing 10 μm. (B) Drug screen utilizing eight different HB cell lines (HB17, 282, 279, 243, 284, 295, 214, HepG2) and one non-HB hepatocyte cell line as control showing panobinostat was associated with the lowest consistent cell viability in all HB cell lines. (C) HepG2, HB17, HuH-6, and HepT1 IC50 of entinostat, panobinostat, vorinostat, and mocetinostat. All cell lines have the lowest IC50 with panobinostat. IC$_{50}$ values were estimated with a nonlinear regression model of log (drug) vs. normalized response, variable slope. (D) PARP cleavage and acetylation of H3/H4 noted when treated with panobinostat 1 μM after 24 h. Acetyl H3/H4 were developed after 100 s of exposure, Total H3/H4 and PARP were developed after 30 s of exposure, and β-actin was developed after 10 s of exposure. HB, hepatoblastoma; PDX, patient-derived xenograft.

chemotherapy, angiogenesis, and migration.[20] Utilizing HDAC inhibition for HB has been suggested since 2016 when *HDAC1* and *HDAC2* overexpression in HB was initially described.[12,21] Previous studies have focused on targeting class 1 HDAC inhibition as a treatment for HB *in vitro*.[12,13] In addition, high *HDAC1* expression has been correlated with worse prognosis in HCC.[22] Apart from validating that class 1 HDAC expression is elevated in high-risk HB, we report a novel elevated pan-HDAC expression, and most notably statistically significant

elevated *HDAC11* expression. While not well described in HB, evidence exists that *HDAC11* expression is directly correlated with disease progression.[22,23] Knockout models of HDAC11 in HCC have been shown to decrease aggressiveness of tumors.[23] While we did not find statistically significant elevation of every HDAC gene, we have shown elevated HDAC class I-IV expression which was validated by RNA sequencing and IHC. Furthermore, we believe that given published literature showing elevated HDAC expression in multiple patient cohorts, targeting
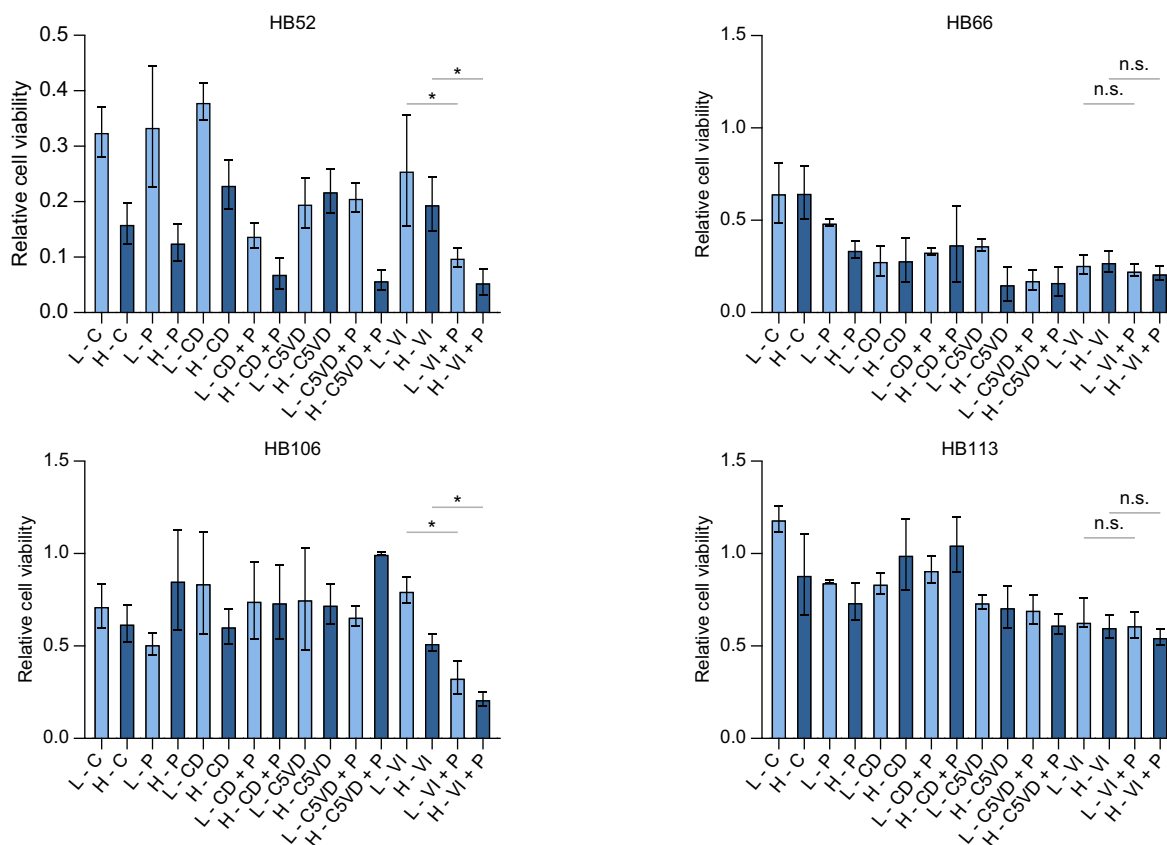
Fig. 3. Vincristine, irinotecan, panobinostat are most effective in HB PDSp. Drug screen of PDSp utilizing standard HB chemotherapy schemes and in combination with Panobinostat, demonstrating VIP was associated with the lowest relative cell viability in three of the four PDSp (HB52, HB106, and HB113). The cell viability in HB52 and HB106 PDSp was statistically lower in the low-dose VIP-treated cohort compared to the low-dose VI-treated cohort. The cell viability in HB52 and HB106 PDSp was also statistically lower in the high-dose VIP-treated cohort compared to the high-dose VI-treated cohort. The drug screen that used low dose (0.05 μM) of each drug is in solid bars and the high dose (0.10 μM) is shown in the checkered bars. Panobinostat was used at 0.01 μM for low dose and 0.05 μM for high dose in all combination studies. SN-38, the active metabolite of irinotecan, was utilized in this assay. Statistical significance was calculated utilizing Student's *t* test (two-tailed) with $p \leq 0.05$ denoted by an asterisk (*) and $p > 0.05$ denoted by n.s. *HB52 PDSp y-axis is adjusted to emphasize the difference in efficacy between the different therapies. C, cisplatin; CD, cisplatin/doxorubicin; CD+P, cisplatin/doxorubicin/panobinostat; C5VD, cisplatin/5-FU/vincristine/doxorubicin; CRVD+P, cisplatin/5-FU/vincristine/doxorubicin/panobinostat; H, high dose; L, low dose; P, panobinostat; PDSp, patient-derived spheroids; VI, vincristine/SN-38; VIP, vincristine/SN-38/panobinostat.

pan-HDAC expression should be considered for all patients with HB.

To evaluate the role that HDAC inhibition plays in HB, we chose to test HDACi that have been or are currently being tested in phase I clinical trials in children[11,24–26]. We found that panobinostat (pan-HDACi) was associated with lower HB cell viability than entinostat (HDAC class I inhibitor), mocetinostat (HDAC class I, IV inhibitor), and vorinostat (HDAC class I, II, and IV inhibitor) in multiple cell lines.[24–26] Furthermore, panobinostat monotherapy was validated by protein immunoblotting and has been shown to cleave PARP during acetylation of both H3 and H4 in HB. Despite this strong efficacy with panobinostat monotherapy, the combination therapy of VIP consistently leads to the lowest cell viability in three high-risk PDSp (HB52, HB66, and HB106). While this finding builds on previous data showing the potential of panobinostat in combination with standard chemotherapy in HB, we demonstrate that the VIP combination appears to have the highest efficacy *in vitro*.[12,13] We hypothesize that this combination therapy likely enhances the apoptotic effect of VI given previous literature demonstrating that panobinostat and

other HDACi lead to potentiation of apoptosis when utilizing cisplatin and other chemotherapy agents.[27,28]

To validate the therapeutic potential that the combination therapy of VIP has, we tested this regimen on four chemo-resistant orthotopic PDX models of HB that we developed in our lab. The lack of clinically relevant models has limited the potential to effectively test therapies for patients with HB.[5] In addition, previous studies that focus on therapies for HB have mainly tested monotherapies instead of focusing on combination therapies *in vivo*.[29] This tasks clinicians with the difficult decision of randomizing patients to a sole small molecule inhibitor arm or utilizing it in combination with a standard chemotherapy scheme.[29] The former risks the chance of limited efficacy while the latter is inadequate by not providing preclinical data. In our study, we demonstrated treatment resistance to panobinostat monotherapy in two of our four PDSp models (HB106 and HB113) and in our HB52 PDX model. In addition to this, previous phase II clinical trials have shown that panobinostat monotherapy has limited efficacy.[11] Given our results and previous literature, we chose to focus on

Table 2. High-risk PDX library.

Model	HB52	HB66	HB106	HB113
Patient				
Sex	F	M	M	F
Race	Hispanic	Hispanic	White	Hispanic
Premature	No	No	No	Yes
Age at diagnosis	12 months	36 months	84 months	46 months
Risk category	HR	HR	HR	Relapse
Surgical treatment	Transplant	Resection	Resection	Transplant
Mets at diagnosis	Yes	Yes	No	Yes
PRETEXT	4	4	3	4
Focality	Multifocal	Multifocal	Multifocal	Multifocal
Tumor rupture	No	No	Yes	No
V+/P+	No	Yes	Yes	Yes
Neoadjuvant chemo	Yes	Yes	Yes	Yes
Total cycles of chemo	6	21	5	9
Chemo regimen before tissue obtained	None	3 Cis, 1 C5VD, 1 VIT	3 Cis/Dox	3 Cis/Dox, 3 Carbo/Dox, 4 VI
Chemo regimen after tissue obtained	6 Cis/Dox/Carboplatin	16 VIT	2 VI	2 VI
RECIST response	Partial response	Stable response	Stable response	Stable response
Pathologic response	99% viable	50% viable	70% viable	100% viable
AFP response after neoadjuvant chemotherapy	99% decrease	700% increase	No change	136% increase
Pathology	Mixed	Mixed	HCN	Mixed
B-catenin	Yes (nuclear)	Yes (nuclear)	Yes (nuclear)	Yes (nuclear)
GPC3	Yes	Yes	No	Yes
Macrovascular invasion	NA	Yes	Yes	No
Microvascular invasion	NA	Yes	Yes	No
Viable nodules	NA	Yes	Yes	NA
CTNNB1 (Tier I) mutation	c.13+158_241+99del	c.53_241+84del	c.A5_A80del	c.17_100del
Tier I/II mutation	NA	*ARID1A* mut, MDM4 amp	RPS6KA3 mut	*SMARCB1* mut
PDX				
PDX origin	Biopsy	Liver tumor (PH)	Liver tumor (PH)	Metastectomy
Engraftment time	3 weeks	2 weeks	3 weeks	2 weeks
Patient AFP	High	High	High	High
PDX AFP	High	High	High	High
Patient metastases	Yes	Yes	Yes	Yes
PDX metastases	Yes	Yes	Yes	Yes
PDX matches patient mutation	Yes	Yes	Yes	Yes

The demographics, tumor/patient characteristics, treatment scheme, and outcomes of relapse/metastatic/treatment-refractory patients that were used to create the PDXs utilized in the study. RECIST was utilized in evaluating tumor response to chemotherapy. The comparisons of the patients to their matched PDXs are also noted.
HB, hepatoblastoma; PDX, patient-derived xenograft.

combination therapy testing. We present in our manuscript four high-risk, aggressive, and orthotopically implanted models that we have utilized to extensively test the VIP combination therapy. These PDXs were extensively validated and found to have identical genetic mutations, β-catenin/glypican 3 staining, and

STR testing as the patients. We treated these mice when they had reached high tumor burden with the goal of providing preclinical data for a new clinical trial arm.

The utilization of irinotecan-based therapy for patients with high-risk disease has been established since 2012.[30] While
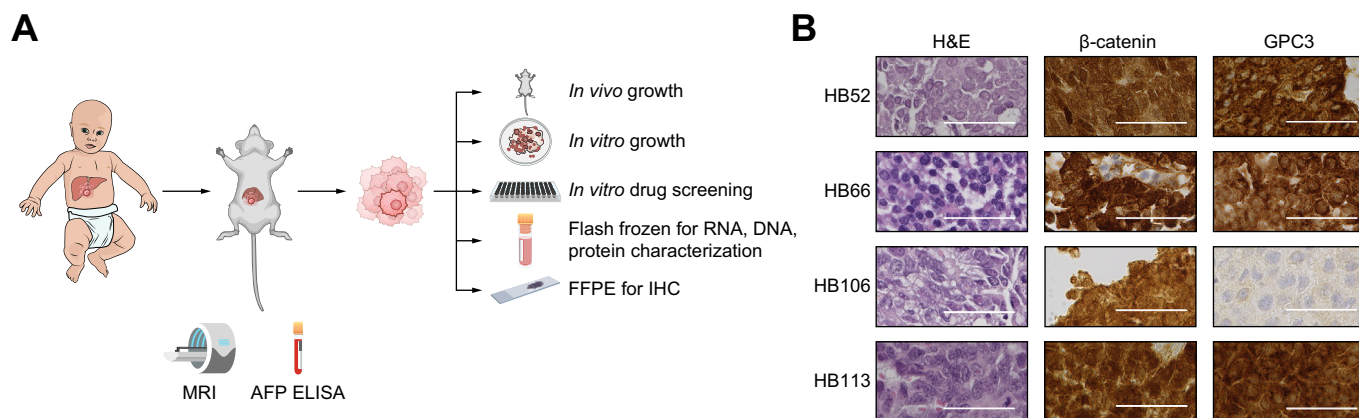

Fig. 4. PDX pipeline development and validation. (A) The pipeline of tumor evaluation, drug testing and PDX creation. (B) The H&E, β-catenin, and GPC3 staining of the PDXs. The images were taken at 40x magnification with the white scale bar representing 50 μm. All four PDXs were noted to have intracellular β-catenin staining. ELISA enzyme-linked immunosorbent assay; MRI, magnentic resonance imaging; PDX, patient-derived xenograft; MRI, magnentic resonance imaging.
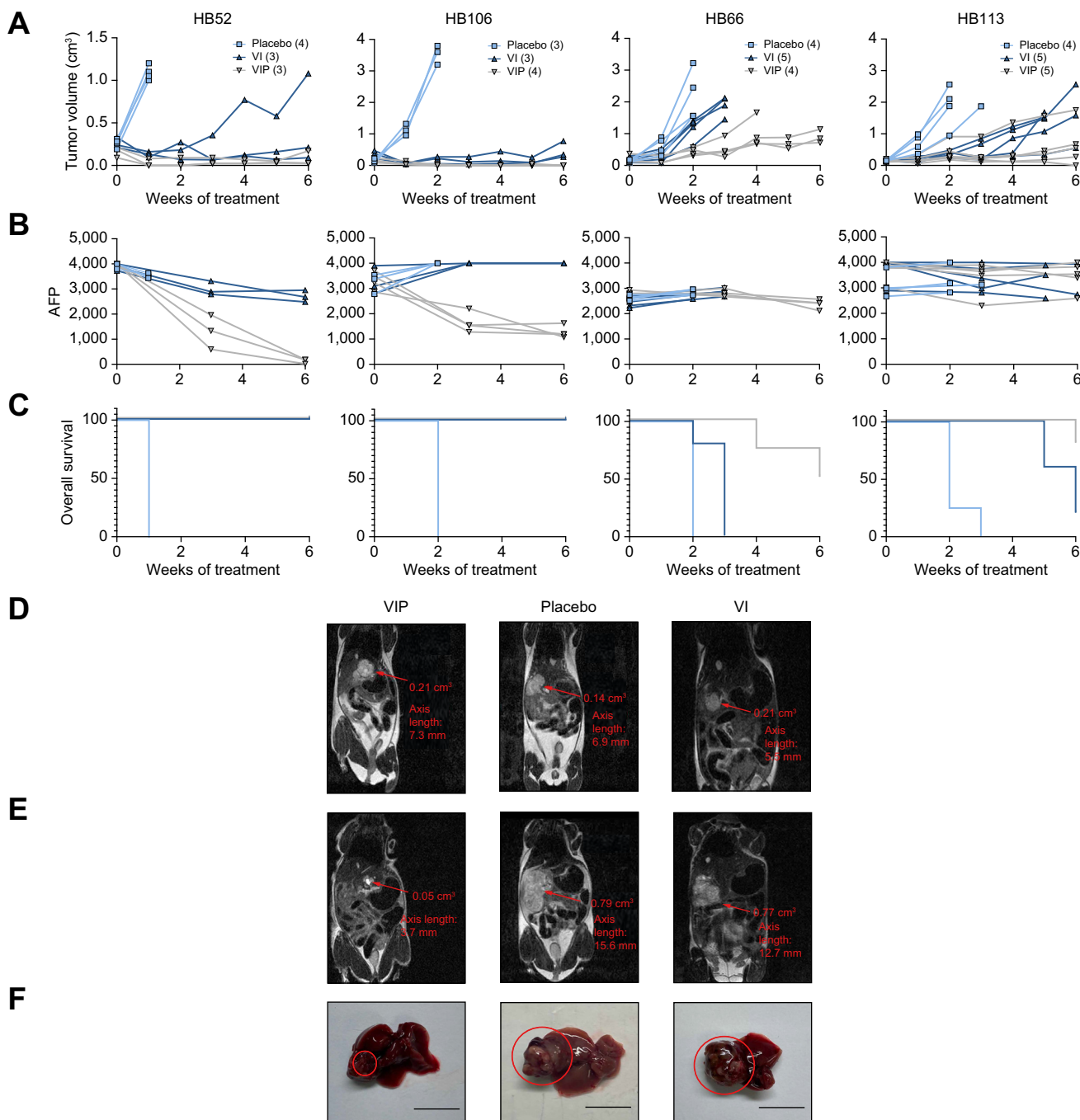
Fig. 5. VIP treatment results in tumor regression or slowing of growth. (A) The comparison of the tumor volume between the three treatment groups of VIP, VI, and placebo over the entire 6-week study in four chemo-resistant PDX models. (B) The progression of AFP in mice over the 6-week study. (C) The KM survival curve over the 6-week study. Parentheses indicate how many mice were included in each cohort. *HB52 tumor volume y-axis is adjusted to emphasize the difference in efficacy between the different therapies. (D) MRI of one of the HB52 placebo-, VI-, and VIP-treated mice tumors at the beginning of the study. (E) MRI of the same mice at time of euthanasia. (F) Explanted livers with tumors (circled in red). The black scale bar represents 1 cm. KM, Kaplan-Meier; PDX, patient-derived xenografts; VI, vincristine/irinotecan; VIP, vincristine/irinotecan/panobinostat.

initially demonstrated to be associated with progression-free survival of 24% at 1 year as monotherapy, the combination with vincristine increased the 3-year event free survival (EFS) rate to 49%.[4,30] Recently, the VI + temsirolimus combination was shown to lead to a similar 3-year EFS rate of 47% with an overall survival rate of 67%.[31] While not improving the EFS of these high-risk patients, this study demonstrated that the addition of an agent to VI is well tolerated. Given this, we believe that a VIP treatment scheme could be proposed as a high-risk arm of a future clinical trial for children with high-risk or relapse/refractory HB who are initially responsive to VI therapy. Currently, in the ongoing clinical trials for pediatric HB, there are no options for children who do not respond to the standard chemotherapy regimens. In our preclinical models we
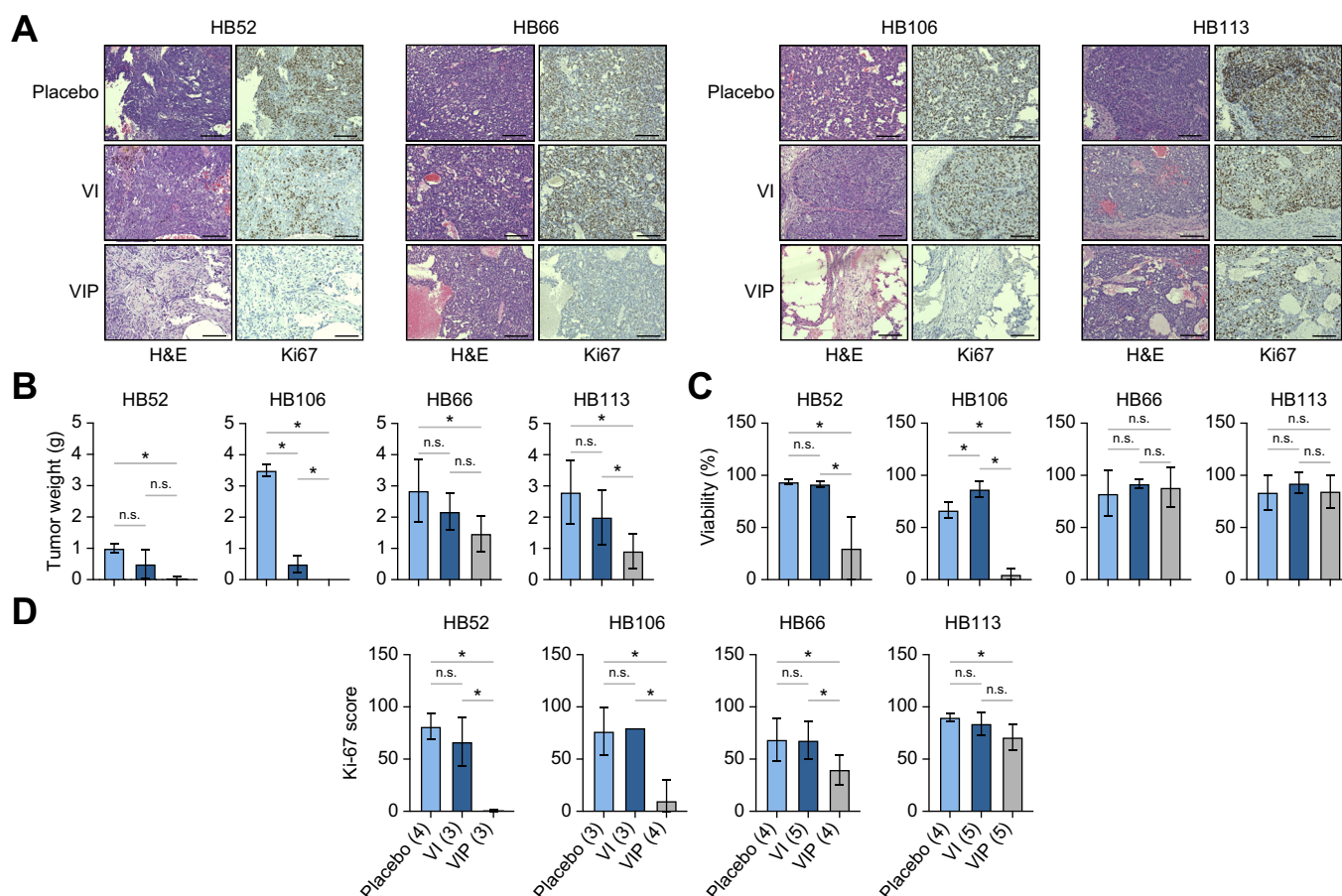
Fig. 6. VIP results in HB tumor necrosis on IHC. (A) The H&E and Ki67 staining of placebo, VI, and VIP group of all four PDX models; (B) tumor weights (C) percent viability, and (D) Ki67 score from placebo, VI, and VIP groups. Percent viability was determined by evaluating manually on H&E. All H&E and Ki67 images were taken at 20x magnification. The black scale bar represents 100 μm. Statistical significance was calculated utilizing Student's t test (two-tailed) with p ≤0.05 denoted by an asterisk (*) and p >0.05 denoted by n.s. VI, vincristine/irinotecan; VIP, vincristine/irinotecan/panobinostat.

have shown that VIP therapy induces cytolytic effects in tumors that are initially responsive to VI (HB52 and HB106). Additionally, we witnessed a complete response to this treatment, with no gross evidence of disease, a decrease in AFP levels in mice, and almost complete tumor necrosis noted on histology. Three of the four PDXs in this study were derived from tumors that were refractory to neoadjuvant chemotherapy. Given that patients with chemo-resistant disease have survival rates that approach 50%, we believe this therapy has the potential to provide patients with a promising treatment option in pursuit of lower rates of relapse and death. Notably, the patients from whom these PDXs were derived were VI naïve and thus likely would have responded similarly to the preclinical models. In contrast, the PDXs that had a significant decrease in tumor volume with the VIP treatment were derived from patients who did not respond to VI (HB66 and HB113). While our study is underpowered to evaluate whether VI therapy response should be used as a screen for patients to receive VIP treatment, further work to identify eligible patients is warranted. This will aid in allowing patient selection if this therapy is included as an arm in clinical trials for treatment-refractory HB. One of the concerns with targeting an epigenetic modulator that has diverse roles is the concern of side effects in patients due to non-specificity. While this may prove to be true in phase II

clinical trials in relapsed/treatment-refractory HB, previous phase I studies have demonstrated minor side effects in the pediatric population.[11] Notably, we have shown in our models that the combination therapy has minor side effects with mice maintaining stable weight throughout the entire study. In addition, the dose that was used for these drug studies is half the human equivalent dose of previous phase I studies.[32] While we believe that our four PDX models have individually demonstrated the efficacy of the VIP combination therapy on high-risk and relapsed/refractory HB, further validation would strengthen our results. We believe that testing this combination therapy on PDX models developed from treatment-refractory tumors acquired through national and international collaborations would further validate the value of this treatment.

To develop further therapies for high-risk HB, evaluating the entire mechanisms of this combination therapy is warranted. We have demonstrated that the addition of panobinostat to VI induced a significant decrease in the HDAC pathway genes, notably decreased expression of the Bcl-2 antiapoptotic family of *BCL2* and *BCL2L1*. While the *BCL2* and *BCL2L1* genetic expression was significantly decreased in all four models with the addition of panobinostat, VI-treated HB66 and HB113 tumors were noted to have the highest level of *BCL2* and *BCL2L1* expression. Interestingly, these two models had the highest

tumor growth throughout the entire 6 weeks of VI treatment. While further validation is warranted, our data suggests that elevated Bcl-2 expression may be correlated with resistance to VI, similar to its correlation with chemoresistance to cisplatin, doxorubicin, and 5-FU.[33,34] In addition, we have shown in our manuscript that panobinostat induces apoptosis in HB *in vitro* and an increase in tumor intensity in T2-weighted imaging after VIP treatment (Fig. 5E), a finding suggestive of necrosis.[23] Nonetheless, we recognize that an epigenetic modulator combined with VI likely leads to multiple pathways being activated. To note, the mechanism of anticancer effects that VI potentiates is not fully understood.[4] We hypothesize that given the synergistic effect of another HDACi (entinostat) and irinotecan previously described, panobinostat and irinotecan may also cause apoptosis through acetylation and thus activation of p53.[35] We recognize that the role of vincristine in relation to both irinotecan and panobinostat warrants further study. In addition, further work to elucidate the cytolytic mechanism in VIP is warranted.

In this study, we continue to strive for an effective and efficient HB preclinical workflow that will provide children with informed therapeutic options before undergoing aggressive treatment. We demonstrate that VIP therapy is an effective treatment strategy that has been validated in four unique chemo-resistant preclinical models, and warrants consideration in future clinical trial arms. In addition, our preclinical testing pipeline can be used to screen new therapies not only for high-risk HB tumors, but for those with unique mutations and characteristics that render them unresponsive to current standard of care treatment regimens.

Affiliations

[1]*Pediatric Surgical Oncology Laboratory, Divisions of Pediatric Surgery and Surgical Research, Michael E. DeBakey Department of Surgery, Texas Children's Surgical Oncology Program, Texas Children's Liver Tumor Program, Dan L. Duncan Cancer Center, Baylor College of Medicine, Houston, TX 77030, USA;* [2]*Department of Pathology and Immunology, Baylor College of Medicine, Texas Children's Department of Pathology, Houston, TX 77030, USA;* [3]*Department of Radiology, Texas Children's Hospital, Baylor College of Medicine, Houston, TX, 77030, USA;* [4]*Pediatric Cancer Biology, Children's Cancer Therapy Development Institute, Beaverton, OR, United States;* [5]*Lester and Sue Smith Breast Center, Baylor College of Medicine, Houston, TX, 77030, USA;* [6]*Department of Pediatrics, Baylor College of Medicine, Texas Children's Hospital and Cancer Center, Houston, TX, USA;* [7]*Department of Pediatrics, Division of Medical Genetics, Duke University, Durham, NC, USA*

Abbreviations

AFP, alpha fetoprotein; EFS, event free survival; HB, hepatoblastoma; HCC, hepatocellular carcinoma; HDAC, histone deacetylase; HDACi, histone deacetylase inhibitors; IHC, immunohistochemistry; PDSp, patient-derived spheroids; PDX, patient-derived xenograft; STR, single tandem repeat; VI, vincristine/irinotecan; VIP, vincristine/irinotecan/panobinostat.

Conflict of interest

The authors declare no competing interests.
    Please refer to the accompanying ICMJE disclosure forms for further details.

Authors' contributions

Conceptualization, A.F.E. and S.A.V.; methodology, A.F.E. and R.H.P.; validation, A.F.E., R.H.P., K.R.P., P.S., S.F.S., M.U., A.M., D.H.L., S.E.W., S.A.V.; formal analysis, A.F.E., K.R.P., R.R.S., B.Z., and S.E.W.; investigation, A.F.E., R.H.P, K.R.P., A.A.B., R.W., R.K.S., S.R.G., A.D., A.K., P.K., B.A., M.T.L, R. R. S., L.E.D., P.S., X.Y., M.J.N.P., B.Z., S.F.S., M.U., A.M., K.B., C.K., D.K., A.H., D.H.L., S.E.W., S.A.V.; resources, R.H.P., D.L.T., S.A.V., and S.E.W.; data curation, A.F.E., R.H.P, K.R.P., A.A.B., R.W., R.K.S., S.R.G., A.D., A.K., P.K., B.A., M.T.L, L.E.D., P.S., X.Y., M.J.N.P., S.F.S., M.U., A.M., K.B., C.K., D.K., A.H., D.H.L., S.E.W., S.A.V; writing—original draft preparation, A.F.E.; writing— review and editing, A.F.E., R.H.P, K.R.P., A.A.B., R.W., R.K.S., S.R.G., A.D., A.K., P.K., B.A., M.T.L, L.E.D., P.S., X.Y., M.J.N.P., S.F.S., M.U., A.M., K.B., C.K., D.K., A.H., D.H.L., S.E.W., S.A.V; visualization, A.F.E.; supervision, D.L.T., S.E.W., S.A.V.; project administration, R.H.P. and S.A.V.; funding acquisition, A.F.E., D.L.T., S.E.W., S.A.V. All authors have read and agreed to the published version of the manuscript.

Data availability statement

RNA sequencing data will be made freely available from the European Archive and Gene Expression Omnibus, under study accession PRJEB64605. NanoString expression estimates are available in the European Archive and Gene Expression Omnibus, under study accession GSE208217.

Supplementary data

Supplementary data to this article can be found online at https://doi.org/10.1016/j.jhep.2024.01.003.

References

Author names in bold designate shared co-first authorship

[1] Musick SR, Smith M, Rouster AS, et al. Hepatoblastoma. In: StatPearls [Internet]. Treasure Island (FL): StatPearls Publishing; 2022 Jan [Updated 2022 Jul 19] Available from: https://www.ncbi.nlm.nih.gov/books/NBK534795/.

[2] Zsiros J, Brugieres L, Brock P, et al. International Childhood Liver Tumours Strategy Group (SIOPEL). Dose-dense cisplatin-based chemotherapy and surgery for children with high-risk hepatoblastoma (SIOPEL-4): a prospective, single-arm, feasibility study. Lancet Oncol 2013 Aug;14(9):834–842. https://doi.org/10.1016/S1470-2045(13)70272-9. Epub 2013 Jul 4. PMID: 23831416; PMCID: PMC3730732.

[3] Sumazin P, Peters TL, Sarabia SF, et al. Hepatoblastomas with carcinoma features represent a biological spectrum of aggressive neoplasms in children and young adults. J Hepatol 2022 Oct;77(4):1026–1037. https://doi.org/10.1016/j.jhep.2022.04.035. Epub 2022 May 14. PMID: 35577029; PMCID: PMC9524481.

[4] Katzenstein HM, Furman WL, Malogolowkin MH, et al. Upfront window vincristine/irinotecan treatment of high-risk hepatoblastoma: a report from the Children's Oncology Group AHEP0731 study committee. Cancer 2017 Jun 15;123(12):2360–2367. https://doi.org/10.1002/cncr.30591. Epub 2017 Feb 17. PMID: 28211941; PMCID: PMC5665173.

[5] Bissig-Choisat B, Kettlun-Leyton C, Legras XD, et al. Novel patient-derived xenograft and cell line models for therapeutic testing of pediatric liver cancer. J Hepatol 2016 Aug;65(2):325–333. https://doi.org/10.1016/j.jhep.2016.04.009. Epub 2016 Apr 23. PMID: 27117591; PMCID: PMC5668139.

[6] Bertacca I, Pegoraro F, Tondo A, et al. Targeted treatment of solid tumors in pediatric precision oncology. Front Oncol 2023 May 5;13:1176790. https://doi.org/10.3389/fonc.2023.1176790. PMID: 37213274; PMCID: PMC10196192.

[7] Foster JH, Voss SD, Hall DC, et al. Activity of crizotinib in patients with ALK-aberrant relapsed/refractory neuroblastoma: a children's oncology group study (ADVL0912). Clin Cancer Res 2021 Jul 1;27(13):3543–3548. https://doi.org/10.1158/1078-0432. CCR-20-4224. Epub 2021 Feb 10. PMID: 33568345; PMCID: PMC8254744.

[8] **Truong DD**, **Lamhamedi-Cherradi SE**, Ludwig JA, et al. Targeting the IGF/PI3K/mTOR pathway and AXL/YAP1/TAZ pathways in primary bone cancer.

J Bone Oncol 2022 Feb 24;33:100419. https://doi.org/10.1016/j.jbo.2022.100419. PMID: 35251924; PMCID: PMC8892134.

[9] Neyns B, Sadones J, Chaskis C, et al. Phase II study of sunitinib malate in patients with recurrent high-grade glioma. J Neurooncol 2011 Jul;103(3):491–501. https://doi.org/10.1007/s11060-010-0402-7. Epub 2010 Sep 25. PMID: 20872043.

[10] McClure JJ, Li X, Chou CJ, et al. Advances and challenges of HDAC inhibitors in cancer therapeutics. Adv Cancer Res 2018;138:183–211. https://doi.org/10.1016/bs.acr.2018.02.006. Epub 2018 Mar 1. PMID: 29551127.

[11] Wood PJ, Strong R, McArthur GA, et al. A phase I study of panobinostat in pediatric patients with refractory solid tumors, including CNS tumors. Cancer Chemother Pharmacol 2018 Sep;82(3):493–503. https://doi.org/10.1007/s00280-018-3634-4. Epub 2018 Jul 9. PMID: 29987369.

[12] Beck A, Eberherr C, Hagemann M, et al. Connectivity map identifies HDAC inhibition as a treatment option of high-risk hepatoblastoma. Cancer Biol Ther 2016 Nov;17(11):1168–1176. https://doi.org/10.1080/15384047.2016.1235664. Epub 2016 Sep 16. PMID: 27635950; PMCID: PMC5137489.

[13] Rivas M, Johnston 2nd ME, Gulati R, et al. HDAC1-Dependent repression of markers of hepatocytes and P21 is involved in development of pediatric liver cancer. Cell Mol Gastroenterol Hepatol 2021;12(5):1669–1682. https://doi.org/10.1016/j.jcmgh.2021.06.026. Epub 2021 Jul 8. PMID: 34245919; PMCID: PMC8536541.

[14] Bär SI, Dittmer A, Nitzsche B, et al. Chimeric HDAC and the cytoskeleton inhibitor broxbam as a novel therapeutic strategy for liver cancer. Int J Oncol 2022 Jun;60(6):73. https://doi.org/10.3892/ijo.2022.5363. Epub 2022 Apr 29. PMID: 35485292; PMCID: PMC9097774.

[15] Kats D, Ricker CA, Berlow NE, et al. Volasertib preclinical activity in high-risk hepatoblastoma. Oncotarget 2019 Nov 5;10(60):6403–6417. https://doi.org/10.18632/oncotarget.27237. PMID: 31741706; PMCID: PMC6849653.

[16] Houghton PJ, Lock R, Carol H, et al. Testing of the topoisomerase 1 inhibitor Genz-644282 by the pediatric preclinical testing program. Pediatr Blood Cancer 2012 Feb;58(2):200–209. https://doi.org/10.1002/pbc.23016. Epub 2011 May 5. PMID: 21548007; PMCID: PMC3154998.

[17] Sumazin P, Chen Y, Treviño LR, et al. Genomic analysis of hepatoblastoma identifies distinct molecular and prognostic subgroups. Hepatology 2017 Jan;65(1):104–121. https://doi.org/10.1002/hep.28888. Epub 2016 Nov 29. PMID: 27775819.

[18] Marks PA. Discovery and development of SAHA as an anticancer agent. Oncogene 2007 Feb 26;26(9):1351–1356. https://doi.org/10.1038/sj.onc.1210204. PMID: 17322921.

[19] Hubbard AK, Spector LG, Fortuna G, et al. Trends in international incidence of pediatric cancers in children under 5 Years of age: 1988-2012. JNCI Cancer Spectr 2019 Mar;3(1):pkz007. https://doi.org/10.1093/jncics/pkz007. Epub 2019 Apr 9. PMID: 30984908; PMCID:PMC6455426.

[20] Witt O, Deubzer HE, Milde T, et al. HDAC family: what are the cancer relevant targets? Cancer Lett 2009 May 8;277(1):8–21. https://doi.org/10.1016/j.canlet.2008.08.016. Epub 2008 Sep 27. PMID: 18824292.

[21] **Clavería-Cabello A**, **Herranz JM**, Latasa MU, et al. Identification and experimental validation of druggable epigenetic targets in hepatoblastoma. J Hepatol 2023 Jun 9;(23):405–411. https://doi.org/10.1016/j.jhep.2023.05.031. S0168–8278 Epub ahead of print. PMID: 37302584.

[22] Quint K, Agaimy A, Di Fazio P, et al. Clinical significance of histone deacetylases 1, 2, 3, and 7: HDAC2 is an independent predictor of survival in HCC. Virchows Arch 2011 Aug;459(2):129–139. https://doi.org/10.1007/s00428-011-1103-0. Epub 2011 Jun 29. PMID: 21713366.

[23] Kim SY, Kim EK, Moon HJ, et al. Association among T2 signal intensity, necrosis, ADC and Ki-67 in estrogen receptor-positive and HER2-negative invasive ductal carcinoma. Magn Reson Imaging 2018 Dec;54:176–182. https://doi.org/10.1016/j.mri.2018.08.017. Epub 2018 Aug 30. PMID: 30172938; PMCID: PMC7383359.

[24] Bukowinski A, Chang B, Reid JM, et al. A phase I study of entinostat in children and adolescents with recurrent or refractory solid tumors, including CNS tumors: trial ADVL1513, Pediatric Early Phase-Clinical Trial Network (PEP-CTN). Pediatr Blood Cancer 2021 Apr;68(4):e28892. https://doi.org/10.1002/pbc.28892. Epub 2021 Jan 12. PMID: 33438318; PMCID:PMC9176707.

[25] Fouladi M, Park JR, Stewart CF, et al. Pediatric phase I trial and pharmacokinetic study of vorinostat: a Children's Oncology Group phase I consortium report. J Clin Oncol 2010 Aug 1;28(22):3623–3629. https://doi.org/10.1200/JCO.2009.25.9119. Epub 2010 Jul 6. PMID: 20606092; PMCID: PMC2917318.

[26] Federman N, Crane J, Gonzales AM, et al. A phase I dose-escalation/expansion clinical trial of mocetinostat in combination with vinorelbine in adolescents and young adults with refractory and/or recurrent rhabdomyosarcoma: interim results. J Clin Oncol 2022;40(16_suppl):11553. 11553.

[27] Takada Y, Gillenwater A, Ichikawa H, et al. Suberoylanilide hydroxamic acid potentiates apoptosis, inhibits invasion, and abolishes osteoclastogenesis by suppressing nuclear factor-kappaB activation. J Biol Chem 2006 Mar 3;281(9):5612–5622. https://doi.org/10.1074/jbc.M507213200. Epub 2005 Dec 23. PMID: 16377638.

[28] Rikiishi H, Shinohara F, Sato T, et al. Chemosensitization of oral squamous cell carcinoma cells to cisplatin by histone deacetylase inhibitor, suberoylanilide hydroxamic acid. Int J Oncol 2007 May;30(5):1181–1188. PMID: 17390020.

[29] Zhong L, Li Y, Xiong L, et al. Small molecules in targeted cancer therapy: advances, challenges, and future perspectives. Signal Transduct Target Ther 2021 May 31;6(1):201. https://doi.org/10.1038/s41392-021-00572-w. PMID: 34054126; PMCID: PMC8165101.

[30] Zsíros J, Brugières L, Brock P, et al. Efficacy of irinotecan single drug treatment in children with refractory or recurrent hepatoblastoma–a phase II trial of the childhood liver tumour strategy group (SIOPEL). Eur J Cancer 2012 Dec;48(18):3456–3464. https://doi.org/10.1016/j.ejca.2012.06.023. Epub 2012 Jul 24. PMID: 22835780.

[31] Thompson PA, Malogolowkin MH, Furman WL, et al. Vincristine/irinotecan/temsirolimus upfront window treatment of high-risk hepatoblastoma: a report from the Children's Oncology Group AHEP0731 Study Committee. Pediatr Blood Cancer 2023 Apr 19:e30365. https://doi.org/10.1002/pbc.30365. Epub ahead of print. PMID: 37073741.

[32] Nair AB, Jacob S. A simple practice guide for dose conversion between animals and human. J Basic Clin Pharm 2016 Mar;7(2):27–31. https://doi.org/10.4103/0976-0105.177703. PMID: 27057123; PMCID: PMC4804402.

[33] Maji S, Panda S, Samal SK, et al. Bcl-2 antiapoptotic family proteins and chemoresistance in cancer. Adv Cancer Res 2018;137:37–75. https://doi.org/10.1016/bs.acr.2017.11.001. Epub 2017 Dec 6. PMID: 29405977.

[34] Geng M, Wang L, Li P, et al. Correlation between chemosensitivity to anticancer drugs and Bcl-2 expression in gastric cancer. Int J Clin Exp Pathol 2013 Oct 15;6(11):2554–2559. PMID: 24228120; PMCID: PMC3816827.

[35] Marx C, Sonnemann J, Beyer M, et al. Mechanistic insights into p53-regulated cytotoxicity of combined entinostat and irinotecan against colorectal cancer cells. Mol Oncol 2021 Dec;15(12):3404–3429. https://doi.org/10.1002/1878-0261.13060. Epub 2021 Jul 29. PMID: 34258881; PMCID:PMC8637561.